PCCP

Physical Chemistry Chemical Physics

www.rsc.org/pccp

Volume 14 | Number 10 | 14 March 2012 | Pages 3261–3696

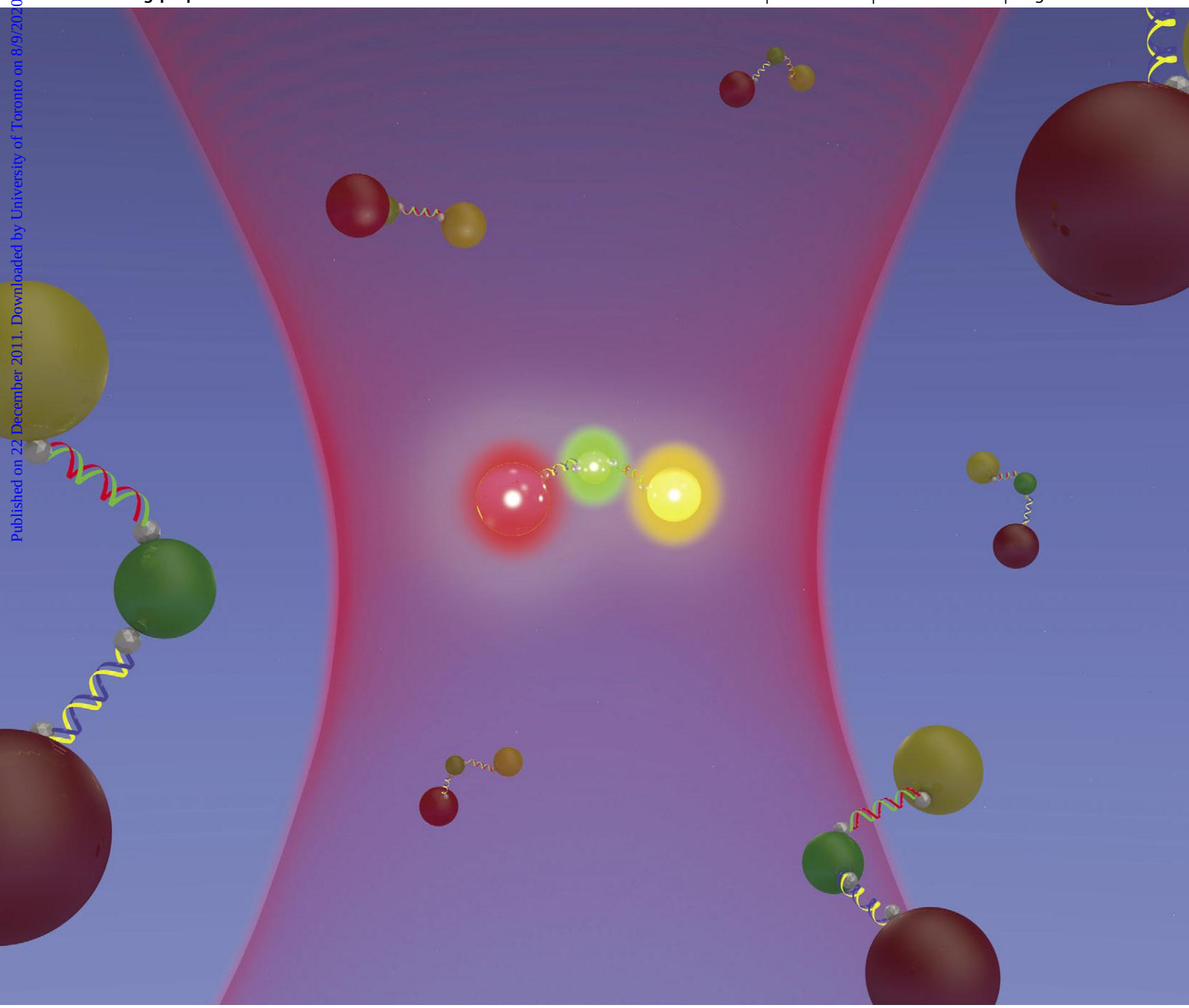

ISSN 1463-9076

COVER ARTICLE
Cramb *et al.*
The development of direct multicolour fluorescence cross-correlation spectroscopy: Towards a new tool for tracking complex biomolecular events in real-time

HOT ARTICLE
Gong *et al.*
Superior reactivity of skeletal Ni-based catalysts for low-temperature steam reforming to produce CO-free hydrogen

PCCP

Cite this: *Phys. Chem. Chem. Phys.*, 2012, **14**, 3290–3294

www.rsc.org/pccp

COMMUNICATION

The development of direct multicolour fluorescence cross-correlation spectroscopy: Towards a new tool for tracking complex biomolecular events in real-time

Holly M. Wobma,†[a] Megan L. Blades,[a] Ekaterina Grekova,[a] Dylan L. McGuire,[b] Kun Chen,[c] Warren C. W. Chan[c] and David T. Cramb*[a]

Received 17th October 2011, Accepted 22nd December 2011
DOI: 10.1039/c2cp23278b

Direct three-colour fluorescence cross-correlation spectroscopy can reveal interactions between three fluorescently labelled biomolecules, giving insight toward the complex events that constitute signal transduction pathways. Here we provide the optical and theoretical basis for this technology and demonstrate its ability to detect specific biological associations between nanoparticle-labelled DNA molecules.

With the completion of the Human Genome Project, current focus has shifted to proteomics, with proteins being at the forefront of cellular and physiological activity. Although expression analysis can suggest likely activities in which a protein is involved, to truly understand their individual functions, one must recognize that they act in concert, with an individual protein being a single player in a complex string of events.[1,2] It is thus necessary to have techniques that detect how and when they interact. Currently, fluorescence-based techniques are available that report association between fluorescently labelled biological molecules. These are Förster Resonance Energy Transfer (FRET), as well as dual-colour fluorescence cross-correlation spectroscopy (FCCS).[3–6] The first achieves this by tracking changes in fluorescence intensity of donor or acceptor molecule due to nonradiative energy transfer, the second, due to a time correlation between the diffusion patterns of linked fluorescent species.

Both FRET and two-colour FCCS (2CFCCS) can only accurately and easily reveal the association between two differently labelled molecules. However, there are many pathways where at least three different molecules interact simultaneously, often, due to one molecule exchanging a molecular partner for another.[7] To capture these complex dynamics, a technique is needed that can detect and quantify the association between three fluorescent species—something that would be very challenging to achieve accurately with FRET.[8] Nevertheless, there is great potential for the development of three-colour FCCS (3CFCCS). As with 2CFCCS, this technique would be based on the fluctuating fluorescence intensities that result from molecules passing in and out of an interrogation volume. If the three different fluorescent species become linked, there would be a mathematical correlation between the intensity fluctuations in each colour channel.

Over the past decade, a model for 3CFCCS has been derived, and the technique has been tested in principle.[9,10] However, these tests have always been based on triple-coincidence analysis.[9] That is, direct real-time triple cross-correlations are not measured and displayed to the user. The reliance on coincidence analysis has likely resulted from the unavailability of an experimental set-up that can cross-correlate more than two fluorescence signals. Here we describe the construction of an apparatus that can achieve direct 3CFCCS and we document the first direct measurement of a 3CFCCS decay. Our technique can provide rapid, real-time analysis of associations between three-species, while simultaneously also providing 2CFCCS and autocorrelation analysis. 3CFCCS remains the only way to confirm directly the existence of species with three colour labels. Moreover, because we are able to calculate and display the two-dimensional 3CFCCS decay (see eqn (1) below), insight is gained into fluctuation dynamics that lead to a 3CFCCS signal. We envision that this technique can be used to track the kinetics of molecular exchanges in signal transduction pathways.

[a] *Department of Chemistry, University of Calgary, 2500 University Dr NW, Calgary, AB, Canada T2N 1N4. E-mail: dcramb@ucalgary.ca; Fax: +1 403 289 9488; Tel: +1 403 220 8138*
[b] *Department of Physics, McGill University, 845 Sherbrooke St. W. Montreal, Quebec, Canada H3A 2T5*
[c] *Institute of Biomaterials and Biomedical Engineering, Donnelly Centre for Cellular and Biomolecular Research, University of Toronto, 160 College St., Toronto, ON, Canada M5S 3E1*

† Contributions to the study: HW – Designed and assembled DNA-QD trimers, collected and analyzed DNA-QD data, contributed to the writing and editing of the manuscript. MB – Designed protocols for, and collected and analyzed nanobead barcode data, contributed to the editing of the manuscript. EG – Designed, wrote and implemented the program for analyzing the correlation data, contributed to the editing of the manuscript. DM – Designed, wrote and implemented the program for collecting the correlation data. KC – Designed and fabricated the barcode nanobeads. WC – Conceived the barcode nanobeads, contributed to the writing and editing of the manuscript. DC – Conceived the study, contributed to all aspects of data analysis and interpretation, contributed to the writing and editing of the manuscript.

The triple cross-correlation function has been previously defined by Schwille and co-workers.[9]

$$G_{3x}(\tau_1,\tau_2) = \frac{\langle \partial F_a(t)\ \partial F_b(t+\tau_1)\ \partial F_c(t+\tau_2)\rangle}{\langle F_a\rangle\langle F_b\rangle\langle F_c\rangle} \quad (1)$$

where the F's are the fluorescence intensities in channels a, b and c. The ∂F's are the instantaneous differences from the time average $\langle F\rangle$'s; the τ's are the lagtimes between the channels. At short lagtimes, the cross-correlation becomes constant, and its amplitude can be related to the average number of triply labelled species in the detection volume.[9]

Since the $G(0)$'s are related to the average number of species occupying the interrogation volume, N, the amplitude of the 3CFCCS function was shown to be:[9]

$$G_{3x}(0,0) = \frac{\langle \partial F_a \partial F_b \partial F_c\rangle}{\langle F_a\rangle\langle F_b\rangle\langle F_c\rangle} = \frac{\langle N_{abc}\rangle}{\left\langle \sum_i N_{ai}\right\rangle\left\langle \sum_j N_{bj}\right\rangle\left\langle \sum_k N_{ck}\right\rangle} = \frac{1}{\langle N_{abc}\rangle^2} \quad (2)$$

where the summations are over all species, i,j,k, that carry the colour label a, b, or c. One can see that a large background of species with one or two colours will lower the 3CFCCS amplitude. The second equality holds true if all the species in solution are trios of a=b=c.

When the fluctuation dynamics are dominated by diffusion through the interrogation volume, the triple-cross correlation matrix is expected to decay to zero with some characteristic time, τ_D.[11] However, the functional form of that decay has not been derived for triple fluorescence correlations. If the behavior is similar to that for quasi elastic light scattering,[12] then the decay of the triple correlation is the product of the dynamics of two pair-wise decays:

$$G_{3x}(\tau_1,\tau_2) = G_{3x}(0,0)M_{ab}(\tau_1)M_{bc}(\tau_2) \quad (3)$$

Where the decay terms are:

$$M_{ab}(\tau) = (1 + \tau_1/\tau_D)^{-1}(1 + r_0^2/\omega_0^2\ \ \tau_1/\tau_D)^{-1/2} \quad (4)$$

$$M_{bc}(\tau) = (1 + \tau_2/\tau_D)^{-1}(1 + r_0^2/\omega_0^2\ \ \tau_2/\tau_D)^{-1/2} \quad (5)$$

where τ_D is the average residence time in the interrogation volume and r_0 and ω_z are the volume depth and waist, respectively. A plot of the cross-correlation matrix (eqn (3)) should show that the variables τ_1 and τ_2 are independent and produce rectangular or square contours. This suggests that the diagonal component of eqn (3) simplifies to:

$$G_{3x}(\tau_1 = \tau_2) = G_{3x}(0,0)M_{ab}^2(\tau) \quad (6)$$

This result would be supported by comparing fits of the decay using eqn (6) to that using the standard correlation decay, the latter of which would have M_{ab} to the first power. We will address both of the above decay issues shortly.

To experimentally realize 3CFCCS, we built an optical setup that simultaneously collects and correlates fluorescence from three colour channels. This set-up is shown in Fig. 1a. Two-photon excitation of fluorophores is achieved using 25 mW (expanded beam to fill the back aperture of the objective lens) 780 nm light pulses of 100 fs duration and 82 MHz repetition rate from a Ti:sapphire laser (Spectra Physics Tsunami pumped by a Spectra Physics Verdi). Although it is possible to do this experiment with one photon excitation,[10] TPE has the advantage of more easily exciting multiple chromophores simultaneously. The light is focused through a c-apochromat (63x, NA 1.2) objective lens mounted on an Axiovert 40 (both from Zeiss, Toronto, Canada). Epifluorescence is collected and directed through a tube lens to an in-house fabricated filter-mounting cube. The fluorescence is spectrally separated by 2 dichroic beamsplitters (565dcxr and Q635lp, Chroma) and directed through notch filters (D500/40, D600/40 and D655/40, Chroma, Bellows Fall, VT) onto optical fibers, which couple the light onto Si avalanche photodiode detectors working in single photon counting mode (Perkin-Elmer, SPCQ-200, Freemont, CA). The signal is directed to an event counter (P7888 multiple event time digitizer, FastComTech, Oberhaching, Germany), which synchronously logs the arrival times of the photons in each of the three channels. We have developed software (C++/CLI) to bin the spectrally separated counts at arbitrary time resolution and simultaneously calculate autocorrelation decays, 2CFCCS decays, and 3CFCCS decays. These are then plotted and outputted as ASCII files.

As test particles to verify the direct measurement of a three-colour FCCS signal, we chose 330 nm diameter polystyrene beads loaded with quantum dots (QDs) of emission wavelengths of 525, 600 and 665 nm. The excellent spectral separation of QDs (shown in Fig. 1b) has the advantage of minimizing spectral cross-talk, which would obfuscate cross-correlation analysis. Since each bead has an average of one of all three colours of QD, they should all deliver a 3CFCCS signal.[13] We note that it is possible to use organic dyes for 3CFCCS.[9,10] Since these dyes have significant spectral tails to longer wavelength, the effect of cross-talk on the cross-correlation must be calculated, as has been previously shown.[9,10]

A schematic representation of the beads is shown in the inset of Fig. 1c. They were prepared as follows. 2.5×10^{11} beads (Bangs Laboratories, Cat. # PC02N, avg. diameter of 330 nm) were mixed with 5 mL of 50% isopropanol with gentle stirring. 30 μL of ZnS/CdS/CdSeS QDs (λ_{em} = 665 nm, 22 μM in chloroform, from Cytodiagnostics, Cat. # FN-665-A) were then added and incubated for 1 h at room temperature. 5 μL of ZnS/CdSe QD (λ_{em} = 600 nm, 22 μM in chloroform) and 25 μL of QD (λ_{em} = 525 nm, 55 μM in chloroform) were then added, and the mixture was incubated for another hour at room temperature. These ZnS/CdSe QDs were synthesized according to methods previously described.[14] After incubation, the beads were centrifuged at 1000 × g for 30 min. The pellet was washed with water using repeated centrifugation cycles.

For 3CFCCS analysis, the beads were dispersed in ultrapure, deionized water to ~0.1 nM. Such a low concentration was adequate for the experiments, because of the particle's high brightness. A typical three-colour count rate trajectory is displayed in Fig. 1c. 3CFCCS decays were calculated, binning at 0.1 ms time resolution. The 3CFCCS decays for five different dilutions of beads are shown in Fig. 1d. These dilutions were chosen to examine the validity of eqn (2), which

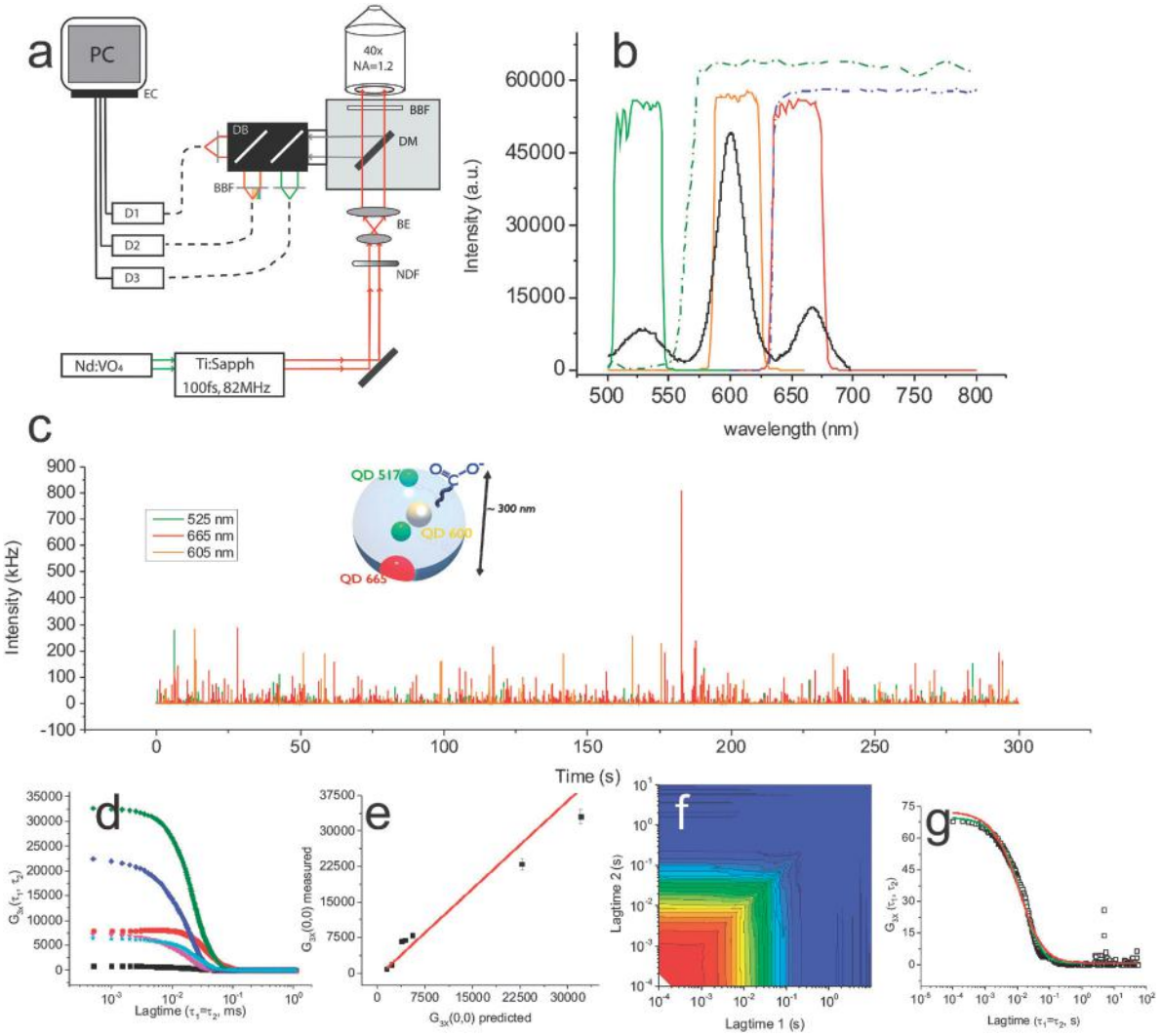

Fig. 1 Three-colour fluorescence cross-correlation spectroscopy of quantum dot barcoded nanobeads. (a) Schematic diagram of the instrumental set-up for 3CFCCS. Included are neutral density filter (NDF), beam expander (BE), dichroic mirror (DM), bandpass barrier filters (BBF), dichroic beamspliters (DB), Si:avalanche photodiode detectors (D) and event counter (EC). (b) Optical spectra of the barcoded nanobead with the spectra of the dichroic beamsplitters (dashed lines) and bandpass barrier filters (solid lines). (c) Fluorescence count rate trajectories for nanobeads under two-photon excitation at 780 nm. Inset is a schematic representation of the nanobead. (d) Various plots of the 3CFCCS decays for the nanobeads. (e) Plot of the predicted (using eqn (2)) *versus* measured amplitudes of the triple cross-correlation. Error bars represent the standard deviation of the fit with eqn (6). The red line represents the best slope (~1). (f) Contour plot of the full 3CFCCS matrix. The plateau amplitude is approximately 150 and the contour lines are 10 units. (g) Fits to the diagonal 3CFCCS decay using eqn (6) (green) or the decay function for the 2CFCCS decay (red). See text for details.

predicts the relationship between particle concentration and correlation amplitude.

In Fig. 1e, a comparison between the measured and predicted values of $G_{3x}(0,0)$, based on eqn (2), is shown. Briefly, the measured fluorescence count rates are used as independent relative measures of N_{abc}. The relative N^2_{abc} values were used to generate predicted relative $G_{3x}(0,0)$ values. These $G_{3x}(0,0)$ values were plotted against the measured values in Fig. 1e. The correlation has an R^2 of 0.98. This suggests that eqn (2) is a valid interpretation of the 3CFCCS amplitude. Moreover, this demonstrates that the relative intensities of the count rate trajectories do not significantly affect the correlation amplitudes. In fact, it is the signal-to-noise ratio (S/N) of each trajectory that is most important.

Fig. 1f shows a plot of the full 3CFCCS matrix for the three-colour beads. The square shape of the contour plot indicates that τ_1 and τ_2 are independent. This indicates that the decays of the correlation with respect to τ_1 and τ_2 can be modeled as a product of the two individual decays as was shown in eqn (3)–(6). Interestingly, this plot is symmetric about the diagonal as one would expect if the decay is dominated by Brownian motion.

As further verification of the independence of τ_1 and τ_2, Fig. 1g shows a fit of the data using eqn (6) (green) *versus* that for the standard decay used in 2CFCCS (red). Inspection by eye and chi-squared values suggest that eqn (6) better represents the data. The better fit returns a residence time of 60 ms, which can be used to calculate the diffusion coefficient, $D = r_0^2/4\tau_D$.[15]

With an r_0 value of 0.2 μm, the diffusion coefficient is 0.16×10^{-12} m^2 s^{-1}. Using the Stokes–Einstein relation, this suggests a hydrodynamic radius of 120 nm, which is close to the value derived using dynamic light scattering (DLS) (165 nm).

Confident that our 3CFCCS instrument was returning reasonable data, we endeavored to measure a more biologically relevant system. It has been demonstrated that multimers of QDs can be assembled using DNA oligonucleotides.[16–18] For the present study, formation of QD-DNA trimers was a two-stage process, involving the conjugation of QDs to single DNA strands via biotin-streptavidin biochemistry and then the hybridization of these QD-DNA conjugates to form trimers. To achieve conjugation, each individual colour of streptavidin-coated QD (525 nm, 605 nm, 655 nm) was added to a specific strand of biotinylated ssDNA in a 1 : 1 ratio in NEBuffer4 1 × (50 mM potassium acetate, 20 mM Tris acetate, 10 mM magnesium acetate, 1 mM DTT, pH 7.9 @ 25 °C), with the QDs and DNA at a concentration of 100 nM in a final total reaction volume of 100 μL. Naturally, the middle QD (525 nm) was mixed with two different (non-complementary) single strands, to allow it to bind to both the outer two QDs (see inset Fig. 2a). The single strand versions of the two DNA sequences used are shown below:

Sequence 1: 5′-Biotin-ACA CAC GAC GGA TCC AGC-3′

Sequence 2: 5′-Biotin-GCA TTA AAG AAT TCA AAA-3′

Sequence 1 and its complement were used to link the 655 nm and 525 nm QDs, and Sequence 2/complement were used to link the 525 nm and 605 nm QDs. Upon adding the DNA and QDs together, the solutions were vortexed for 1 h on a low setting to promote mixing. To then make the trimer assemblies, the full contents of all three QD-DNA reaction tubes were mixed and allowed to vortex for another hour. This created a trimer mixture with a concentration of 33 nM for each QD, which could be diluted to the desired final concentration (~10 nM) using NEBuffer.

The inset of Fig. 2a displays the count rate trajectories for putative trimers. Note that the red channel is considerably brighter than the orange and green, consistent with the brightnesses of the individual QDs. Fig. 2a shows the 3CFCCS decay of the trimer solution. The value of $G_{3x}(0,0)$ was used to calculate the average concentration of triply labeled DNA associates. An average concentration of 12 nM was found for the three-coloured species. We expect some heterogeneity in the sample solution because the three-colour assembly will be a statistical distribution, *i.e.* some assemblies will not be 1 : 1 : 1 (QD500 : QD605 : QD655). Unfortunately, it is not possible to extract the distribution from the correlation amplitudes mathematically. Nevertheless, a fit to the data (Fig. 2a) delivers a residence time of 0.020 ms, which converts to a hydrodynamic diameter of 80 nm. This is consistent with the size of a linear trimer (DLS sizing: QDs 20 nm diameter, DNA ~6 nm).

A full 2-D contour plot of the 3CFCCS data is presented in Fig. 2b. The contours are perpendicular (within the noise limit of the data) with respect to the two lagtimes. This suggests, again, that the lagtimes are independent of each other. However, unlike the contour plot for the nanobeads, the plot is not symmetrical about the equal lagtime diagonal. This is an interesting result, because it cannot be explained using

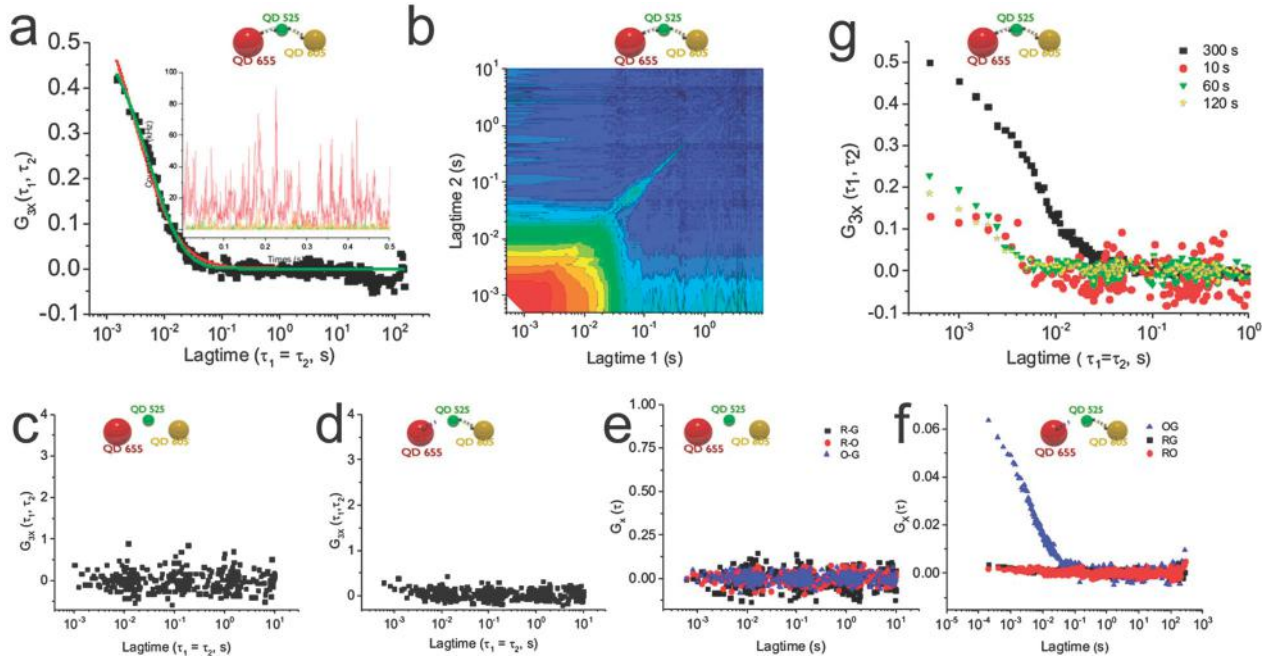

Fig. 2 3CFCCS of DNA assembled three-colour QD trimers. (**a**) 3CFCCS decay of ~10 nM solution of trimers. The green line is a fit to the data using eqn (6) whereas the red line is a fit using the 2CFCCS decay. Insets show the fluorescence count rate trajectories and schematic diagram of the trimer. (**b**) Contour plot of the full 3CFCCS matrix for the solution described in above. The amplitude is 0.5 and the contour lines are 0.065 units apart. (**c**) and (**e**) are the 3CFCC and 2CFCC decays, respectively of a solution of the three QDs used in the trimer. Note that no correlation was observed. (**d**) and (**f**) are the 3CFCC and 2CFCC decays, respectively of a solution of the trimer assembly with one DNA strand missing (see text). Note that there is substantial amplitude only for the expected dimer cross-correlation. (**g**) A time series from the solution examined in panel a). These plots represent the 3CFCCS decay calculated after 10, 60, 120 and 300 s collection time. Good signal to noise is apparent after 60 s.

diffusion dynamics. The rectangular shape may result from photophysical interactions between the QDs on msec timescale and is the subject of a future study.

To verify that the trimer QD-DNA assemblies are specifically created through DNA linkage rather than nonspecific adherence of QDs to each other, control experiments were performed. In the first, an equivalent trimer mixture of QDs was generated in the absence of DNA. The resulting solutions produced no cross-correlations (Fig. 2c and e). In a second control, QDs were incubated with DNA as above, but with the complementary strand for the red-green connection missing. The resulting cross-correlation decays are shown in Fig. 2d and f. Significant amplitude was only observed for the expected 2CFCCS decay for orange-green assemblies. No evidence of FRET was observed in these experiments.

Finally, we examined the utility of the 3CFCCS instrument for dynamics measurements by determining the S/N of the 3CFCCS decay as a function of collection time (Fig. 2g). After only 10 s of data collection, there is sufficient S/N to estimate the $G_{3x}(0,0)$ value. The S/N becomes greater than 4 at 60 s, which is usually sufficient time resolution to measure cellular reaction kinetics at low concentrations. Future studies will examine the sensitivity of TCFCCS to detect trimers with a large background of free quantum dots, but such experiments are beyond the scope of this proof-of-principle correspondence.

Conclusions

We have demonstrated the development and implementation of a fluorescence correlation instrument that directly measures three-colour fluorescence cross-correlation signals. The instrument was tested on barcoded nanobeads containing three different QDs and on trimeric QD assemblies using DNA as linkers. A 3CFCCS decay of the QD-DNA trimer can be measured with good S/N in less than 1 min. This indicates that complex, multipartner biochemical processes can be observed directly, in real time, using 3CFCCS.

Acknowledgements

We are grateful to NSERC and CIHR for funding this research through the AGENO and CHRP programs. MLB and HMW thank NSERC and the University of Calgary, respectively, for scholarship support. The authors are indebted to Professor Simon Trudel (Calgary) for generating the nanoparticle graphics. We are indebted to Andy Read, Joel Schreiner, and Todd Willis for design and fabrication of the detection filter cube.

Notes and references

1 T. Pawson and P. Nash, *Genes Dev.*, 2000, **14**, 1027.
2 X. J. Duan, I. Xenarios and D. Eisenberg, *Mol. Cell. Proteomics*, 2002, **1**, 104.
3 I. Medintz and H. Mattoussi, *Phys. Chem. Chem. Phys.*, 2009, **11**, 17.
4 D. Magde, E. L. Elson and W. W. Webb, *Biopolymers*, 1974, **13**, 29.
5 P. Schwille, F. J. Meyer-Almes and R. Rigler, *Biophys. J.*, 1997, **72**, 1878.
6 R. Oyama, H. Takashima, M. Yonezawa, N. Doi, E. Miyamoto-Sato, M. Kinjo and H. Yanagawa, *Nucleic Acids Res.*, 2006, **34**, e102.
7 S. C. Schuster, R. V. Swanson, L. A. Alex, R. B. Bourret and M. I. Simon, *Nature*, 1993, **365**, 343.
8 S. Hohng, S. Joo and T. Ha, *Biophys. J.*, 2004, **87**, 1328.
9 K. Heinze, M. Jahnz and P. Schwille, *Biophys. J.*, 2004, **86**, 506.
10 L. C. Hwang, M. Gösch, T. Lasser and T. Wohland, *Biophys. J.*, 2006, **91**, 715.
11 J. L. Swift, R. Heuff and D. T. Cramb, *Biophys. J.*, 2006, **90**, 1396.
12 G. D. J. Phillies, *J. Chem. Phys.*, 1980, **72**, 6123.
13 S. Fournier-Bidoz, T. L. Jennings, J. L. Klostranec, W. Fung, A. Rhee, D. Lee and W. C. W. Chan, *Angew. Chem., Int. Ed.*, 2008, **47**, 5577.
14 H. C. Fischer, T. S. Hauck, A. Gómez-Aristizábal and W. C. W. Chan, *Adv. Mater.*, 2010, **22**, 2520.
15 S. T. Hess and W. W. Webb, *Biophys. J.*, 2002, **83**, 2300.
16 A. P. Alivisatos, K. P. Johnsson, X. Peng, T. E. Wilson, C. J. Loweth, M. P. Bruchez Jr. and P. G. Schultz, *Nature*, 1996, **382**, 609.
17 G. P. Mitchell, C. A. Mirkin and R. L. Letsinger, *J. Am. Chem. Soc.*, 1999, **121**, 8122.
18 G. Tikhomirov, S. Hoogland, P. E. Lee, A. Fischer, E. H. Sargent and S. O. Kelley, *Nat. Nanotechnol.*, 2011, **6**, 485.

